Ferroelectric and photocatalytic properties of Aurivillius phase Ca2Bi4Ti5O18

Received: 16 June 2020 | Revised: 9 August 2020 | Accepted: 23 August 2020

DOI: 10.1111/jace.17466

Journal of the American Ceramic Society

ORIGINAL ARTICLE

Ferroelectric and photocatalytic properties of Aurivillius phase $Ca_2Bi_4Ti_5O_{18}$

Yaqiong Wang[1] | **Man Zhang**[1] | **Jiyue Wu**[1] | **Zimeng Hu**[1] | **Hongtao Zhang**[2] | **Haixue Yan**[1]

[1]School of Engineering and Materials Science, Queen Mary University of London, London, UK

[2]Department of Materials, Loughborough University, Leicestershire, UK

Correspondence
Man Zhang, School of Engineering and Materials Science, Queen Mary University of London, Mile End Road, London, E1 4NS, UK.
Email: ma.zhang@qmul.ac.uk

Abstract

Aurivillius phase $Ca_2Bi_4Ti_5O_{18}$ powders with micrometer size were produced by solid-state reaction. X-ray diffraction revealed that the powders had polar orthorhombic structure with space group of *B*2*cb*. $Ca_2Bi_4Ti_5O_{18}$ ceramic exhibited frequency independent dielectric anomaly at 774°C. The piezoelectric coefficient d_{33} value of poled $Ca_2Bi_4Ti_5O_{18}$ pellets was 0.7 ± 0.2 pC/N. Both frequency independent dielectric anomaly and detectable d_{33} value clearly indicated that $Ca_2Bi_4Ti_5O_{18}$ is a ferroelectric material with Curie point of 774 °C. UV–vis absorption spectra revealed that $Ca_2Bi_4Ti_5O_{18}$ had a direct band gap of 3.2 eV. Photocatalytic activity of the $Ca_2Bi_4Ti_5O_{18}$ powders was examined by degradation of rhodamine B (RhB) under simulated solar light. 16% of RhB solution was degraded by $Ca_2Bi_4Ti_5O_{18}$ powders after 4 hours UV-vis irradiation. With Ag nanoparticles deposited on the $Ca_2Bi_4Ti_5O_{18}$ powders surface, 50% of RhB was degraded under the same irradiation condition. The fitted degradation rate constant of Ag decorated $Ca_2Bi_4Ti_5O_{18}$ was 4 times higher than that of bare $Ca_2Bi_4Ti_5O_{18}$. This work suggested that the Aurivillius ferroelectric $Ca_2Bi_4Ti_5O_{18}$ is a promising candidate for photocatalytic applications.

KEYWORDS

Aurivillius phase, $Ca_2Bi_4Ti_5O_{18}$, ferroelectrics, photocatalysts

1 | INTRODUCTION

Aurivillius phase materials (bismuth layer structure ferroelectrics, BLSFs) with the general formula of $(Bi_2O_2)(A_{m-1}B_mO_{3m+1})$ have the crystalline structure that is an intergrowths of fluorite-like $(Bi_2O_2)^{2+}$ layers alternating with perovskite $(A_{m-1}B_mO_{3m+1})^{2-}$ slabs along the crystallographic *c*-axis, where A is a mono-, di-, or/and trivalent ion and B is usually a transition metal ion.[1-3] The integer *m* is the number of octahedral layers in the perovskite slab. The properties of BLSFs could be flexibly adjusted using versatile dopants as well as by changing the layer number, *m*. Aurivillius phase materials are promising candidates for nonvolatile ferroelectric random access memories and high-temperature piezoelectric transducers, due to their excellent fatigue-resistant properties, high Curie point (T_c), as well as their high-temperature stability.[4,5] Moreover, a number of Aurivillius phase compounds, such as $Bi_5Ti_3FeO_{15}$, $Bi_6Ti_3Fe_2O_{18}$, *etc*, exhibit multiferroic properties.[6]

Kikuchi studied structural stability of BLSFs by using an elastic model and reported that increase in *m* causes increasing lattice parameters and elastic strain energy.[7] The large elastic strain energy makes the structure of BLSFs with high *m* value ($m \geq 5$) highly unstable. As a consequence, structurally stable BLSFs with low *m* value ($m \leq 4$), such as Bi_2WO_6 ($m = 1$), $SrBi_2Ta_2O_9$

($m = 2$), $Bi_4Ti_3O_{12}$ ($m = 3$), and $SrBi_4Ti_4O_{15}$ ($m = 4$), have been extensively studied in the last decades.[8] Although the BLSFs with high m value may offer better flexibilities for performance manipulation, very little is known about these compounds due to challenge in the experimental synthesis.[7,9-13]

$Ca_2Bi_4Ti_5O_{18}$ (C2BT) is one of members in the Aurivillius family with $m = 5$. X-ray diffraction (XRD) analysis by different groups indicated that crystal structure of C2BT adopts orthorhombic symmetry with a space group of either *B2cb* or $Bb2_1m$.[14,15] However, there is no general consensus about T_c of C2BT. Based on powder synchrotron XRD results, Ismunandar *et al* found that C2BT showed the orthorhombic structure with a space group of *B2cb* from room temperature to 675 K. Above 675 K the orthorhombic structure was transformed into the tetragonal I4/mmm structure.[14] Hou et al reported that in spite of detectable piezoelectric constant d_{33} of 2 pC/N in poled C2BT ceramic, no dielectric anomaly was observed in the permittivity-temperature curves from room temperature up to 800°C. Thus, they inferred that T_c of C2BT should be above 800°C.[16] Moure and Xu et al evaluated T_c of C2BT to be 775°C from dielectric anomaly in permittivity-temperature curves at a fixed frequency.[15,17]

In addition to aforementioned applications, Aurivillius ferroelectrics, such as $Bi_5Ti_3FeO_{15}$,[18,19] $Bi_4Ti_3O_{12}$,[20] and $PbBi_2Nb_2O_9$,[21] have also been explored as photocatalysts in recent years. Semiconductor photocatalysis technology is promising for environmental remediation and solar energy conversion, such as water disinfection by degradation of hazardous organic pollutants from industrial effluent, hydrogen production by water splitting, *etc* ◦ The electrons and holes can be generated in a semiconductor photocatalyst under super-band-gap irradiation. These photoexcited charge carriers are able to participate in various redox reactions to decompose hazardous organic pollutants and split water to produce hydrogen.[22] The photocatalysis efficiency of traditional semiconductor oxides (TiO_2, ZnO, *etc*) and sulphides (ZnS and CdS) is very low (ca. 10%) due to their large band gap and rapid recombination of photoexcited electrons and holes.[23] Spontaneous polarization in a ferroelectric material can induce the internal depolarization field, which is beneficial to drive the separation of photoexcited charge carriers effectively.[24] Furthermore, as bismuth-containing compounds, BLSFs show superior photocatalytic activity, which can be attributed to: (a) The formation of a hybridized valence band comprising of Bi 6s and O 2p states pushes up the absorption band edge, and thus leads to a reduction in the band gap; (b) The dispersed nature of hybridized valence bands enhances the mobility of the photoexcited holes, and thus facilitates the photodegradation process.[25,26] Moreover, to further improve photocatalytic efficiency, noble metal nanoparticles (such as Ag, Au, Pt, *etc*) are often deposited onto the surface of ferroelectric photocatalysts to form the co-catalyst.[27,28,29] These metal nanoparticles can increase light absorption due to a surface plasmon resonance and extend the charge carrier lifetime by working as "electron traps" to separate photoexcited electrons and holes, which results in improved photocatalytic efficiency.[22,30,31] Compared to ferroelectric photocatalysts with perovskite structure, Aurivillius ferroelectrics with more complex structure remained largely unexplored. Therefore, it is imperative to examine new photocatalysts with Aurivillius phase and the effect of Ag nanoparticle decoration on photocatalytic properties.

Given that there is no agreement in electrical properties of C2BT and no report on photocatalytic properties of C2BT, in this paper we first synthesized C2BT powders by solid-state reaction. The dielectric, ferroelectric and piezoelectric properties of C2BT ceramic were re-investigated. Some of C2BT powders were decorated with Ag nanoparticles (hereafter named as C2BT-Ag) prior to the characterization of photocatalytic properties. Finally, the photocatalytic behaviour of both C2BT and C2BT-Ag powders in the photodegradation of an organic dye, Rhodamine B (RhB), was investigated under simulated solar light.

2 | EXPERIMENTAL PROCEDURE

2.1 | Samples preparation

$Ca_2Bi_4Ti_5O_{18}$ (C2BT) powders were prepared by the conventional solid-state reaction method. Reagent-grade carbonate or oxide powders of $CaCO_3$ (99.9% purity), Bi_2O_3 (99.9%), and TiO_2 (99.5%) were mixed in stoichiometric ratio and ball milled by using zirconia balls in ethanol media for 24 hours. The powder mixture was dried overnight at 80 °C. Different calcination conditions were attempted and the optimal condition was found to be at 950°C for 4 hours. The calcined powders were re-milled in ethanol for 24 hours to reduce the particle size. The as-milled C2BT powders were used for photocatalytic property test and for fabrication of ceramics for electrical property characterization. The as-milled C2BT powders were pressed into cylindrical discs with 10 mm diameter using poly(ethylene glycol) (PEG) as a binder at 150 MPa and sintered at 1100°C for 1 hours in air. The relative density of the C2BT ceramic measured by Archimedes method was ~94%. Ag nanoparticles were deposited onto the surface of the as-milled C2BT powders by following a photoreduction method reported elsewhere.[22,32] In a typical procedure, 0.5 g of C2BT powders were added into a Petri dish with 50 mL of 0.01 M $AgNO_3$ solution. The mixture was placed under a UV source (UV Cube with a high-pressure Hg lamp, Honle) for 10 s under constant stirring. The final products were separated from the solution by centrifuging with a speed of 4000 rpm for 15 minutes. The C2BT-Ag powders were collected after being washed by DI water and dried at room temperature. Prior to electrical property measurement, either Pt or Ag electrode was applied by painting with paste on the polished surfaces of C2BT pellets. In order to enhance adhesion strength between electrode and C2BT pellets, Pt- and Ag-coated C2BT pellets

were fired at 900°C for 10 minutes and 300°C for 30 minutes, respectively. The Pt-coated samples were used to measure temperature and frequency dependence of dielectric properties. The Ag-coated samples were used for poling, ferroelectric and piezoelectric measurement.

2.2 | Characterization

The crystal structure of the as-milled C2BT powders was characterized by XRD (Panalytical Xpert Pro diffractometer, with Cu-K_α radiation). Scanning electron microscope (SEM, FEI Inspect F) equipped with energy dispersive X-ray spectroscopy (EDX) was used to observe the morphology and test chemical composition of ceramic powders. Laser diffraction (Zetasizer Nano, Malvern Instruments Ltd, UK) was used to measure the particle size distribution of the as-milled C2BT powders. The polarization-electric field (*P-E*) and current-electric field (*I-E*) loops were measured using a ferroelectric hysteresis measurement tester (NPL, UK) at 25°C and 10 Hz. The temperature dependence of the dielectric permittivity and loss was measured at different frequencies using an LCR meter (Agilent Technologies Ltd, 4284A, Kobe, Hyogo, Japan) connected to a furnace. C2BT pellets for piezoelectric measurements were poled in silicone oil at 200°C under DC electric field of 13 kV/mm for 10 min. The piezoelectric constant, d_{33}, was measured using a piezo d_{33} meter (ZJ-3B, Institute of Acoustics, Chinese Academic of Science, Beijing). The composition and chemical states in C2BT-Ag powders were detected by X-ray photoelectron spectroscopy (XPS, Thermo Scientific™ Nexsa™, with an Al K_α X-ray source). C1s signal from adventitious carbon with a binding energy of 284.8 eV was used to calibrate all the binding energies. The optical absorption spectra of as-milled C2BT powders were obtained using UV-vis spectrophotometer (PerkinElmer LAMBDA 950). The photocatalytic activity of unpoled C2BT and C2BT-Ag powders was studied by degrading a Rhodamine B (RhB, 99.99%) dye solution under simulated solar light. Photocatalysts powders (150 mg) were mixed with 50 ml of 10 ppm dye solution in a glass Petri dish. The mixture was placed under dark and stirred for 0.5 hour before exposed to the solar simulator (Newport, class ABB). The irradiation intensity was calibrated by a silicon reference solar cell (Newport, Model: 91150 V) to 1 sun (100 mW/cm^2). 2 mL of sample was collected from the solutions every 0.5 hour and centrifuged at 10,000 rpm for 15 minutes in order to remove the photocatalysts powders from the dye solution.

3 | RESULTS AND DISCUSSION

XRD pattern of the as-milled C2BT powders is shown in Figure 1. The diffraction peaks were indexed in orthorhombic

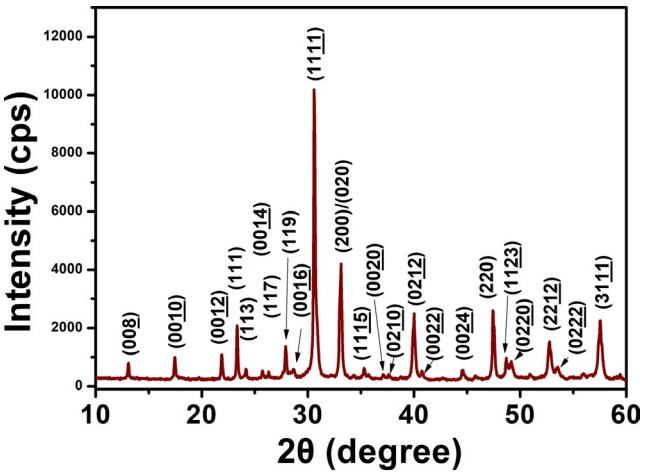

FIGURE 1 X-ray diffraction pattern of as-milled C2BT powders [Color figure can be viewed at wileyonlinelibrary.com]

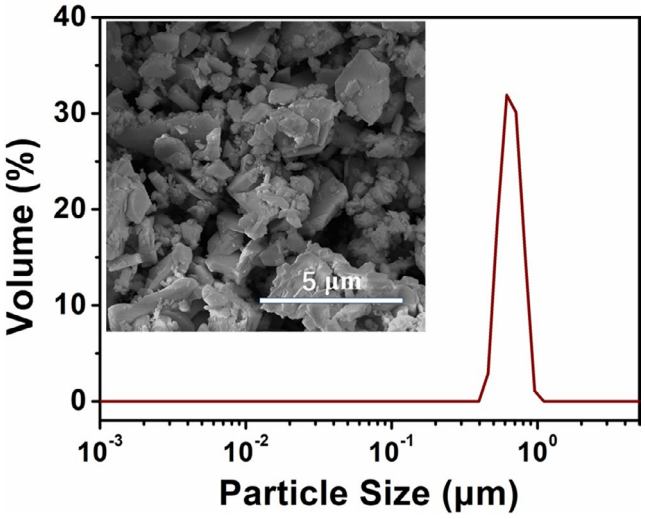

FIGURE 2 Particle size distribution of the as-milled C2BT powders. Inset: scanning electron microscope image of the as-milled C2BT powders [Color figure can be viewed at wileyonlinelibrary.com]

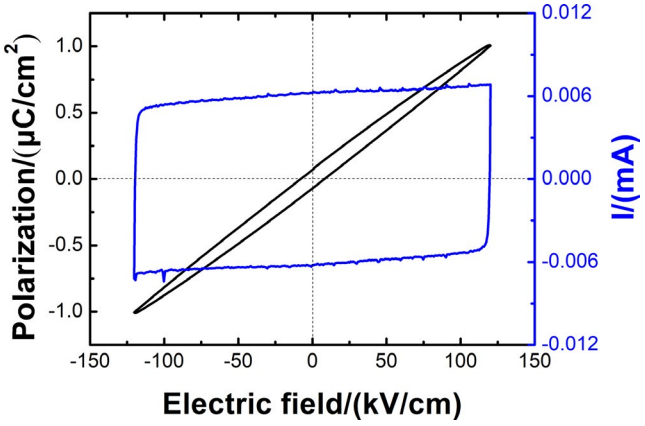

FIGURE 3 Polarization-electric field (*P-E*) and current-electric field (*I-E*) hysteresis loops measured at room temperature [Color figure can be viewed at wileyonlinelibrary.com]

symmetry with space group of *B2cb*, which is in agreement with Ismunandar's work.[14] In addition, the strongest diffraction peak of C2BT powders was (*11* 11), which is consistent with (*11 2m + 1*) highest diffraction peak in Aurivillius phases.[33] Thus, the synthesized C2BT powders consisted of a single Aurivillius phase with $m = 5$.

Particle size distribution of as-milled C2BT powders is shown in Figure 2, which indicates the sizes of majority of the particles were within 0.4-1 μm and a broadened unimodal distribution peak at around 0.6 μm. The as-milled C2BT powders were visualized with SEM (the inset in Figure 2). The most of C2BT powders exhibited an irregular morphology with a broad particle size distribution ranging from 0.3 to 3.0 μm. There were some powders with plate-like morphology, which reflects the anisotropic nature of the crystal structure.

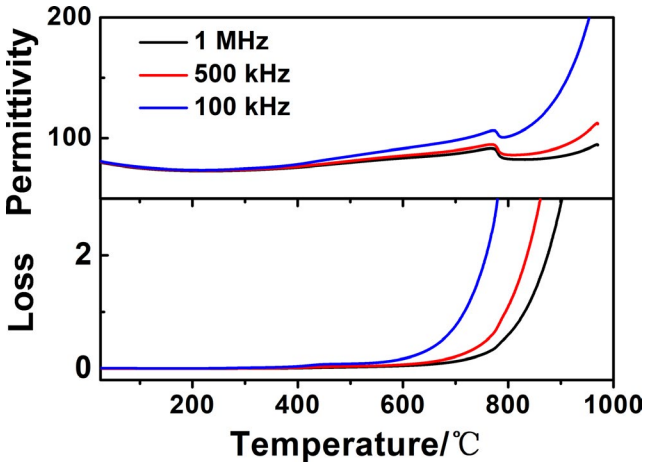

FIGURE 4 Temperature dependence of dielectric permittivities and losses of C2BT ceramic at different frequencies [Color figure can be viewed at wileyonlinelibrary.com]

In order to confirm the ferroelectric nature of C2BT, *P-E* and *I-E* hysteresis loops were measured at 25°C under a maximum applied electric field of 120 kV/cm and 10 Hz (Figure 3). Compared to the maximum electric field (30 kV/cm) applied by Hou *et al* during *P-E* loop measurement of C2BT ceramic at room temperature,[16] the one (120 kV/cm) used in this work is much higher. However, *I-E* loop indicate capacitor behaviour of C2BT ceramic and the onset of ferroelectric domain switching was not observed, which is probably due to very high coercive field of C2BT ceramic.[17] The dielectric permittivity ε_r and loss of C2BT ceramic were measured as a function of temperature at different frequencies ranging from 100 kHz to 1 MHz (Figure 4). The dielectric anomaly, as evidenced by the well-defined frequency independent maximum of ε_r, can be observed at 774°C. When C2BT pellets were poled at 200°C, the d_{33} value of 0.7 ± 0.2 pC/N was obtained. Both frequency independent dielectric anomaly and detectable d_{33} value suggest that C2BT is a ferroelectric. This is consistent with previously reported results by other groups.[15,16,34] But to the best of our knowledge, this is the first time to demonstrate frequency-independent dielectric anomaly of C2BT ceramic.

The chemical species and their chemical states in C2BT-Ag powders were identified by XPS, as shown in Figure 5. The existence of Ca, Bi, Ti, O, and Ag elements was observed from the XPS survey spectrum [Figure 5A]. Figure 5B shows the high resolution XPS spectrum around Ag 3d region for C2BT-Ag powders. The two peaks at 368.28

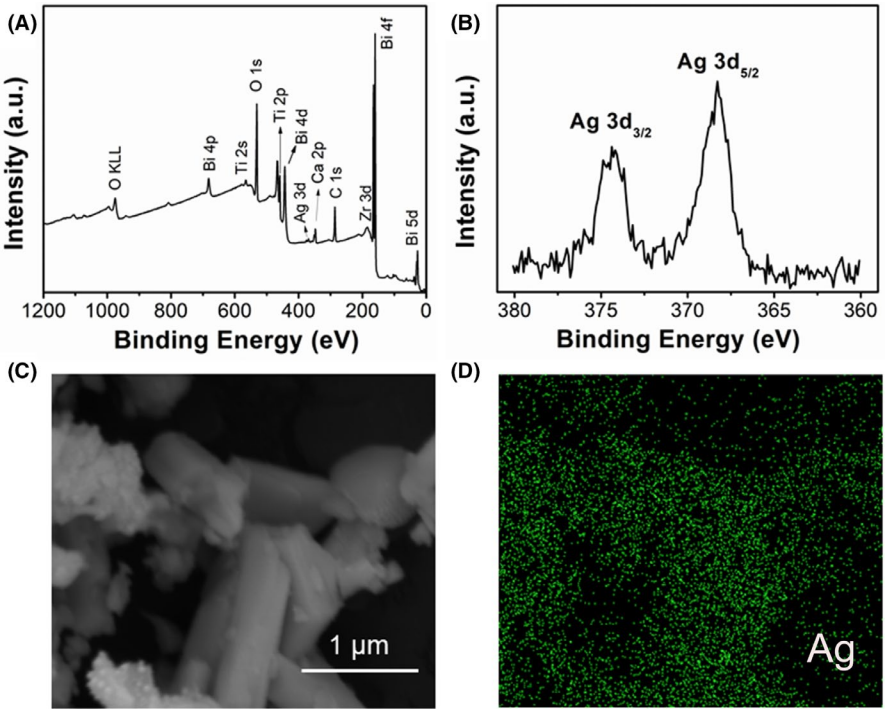

FIGURE 5 Chemical composition/states and morphology of C2BT-Ag powders: (A) X-ray photoelectron spectroscopy (XPS) survey spectra; (B) XPS of Ag 3d spectra; (C) scanning electron microscope; and (D) energy dispersive X-ray spectroscopy mapping of Ag element [Color figure can be viewed at wileyonlinelibrary.com]

and 374.28 eV are characteristic of Ag $3d_{5/2}$ and Ag $3d_{3/2}$, respectively. The spin-orbit splitting energy of the 3d doublet is 6.0 eV. The difference of binding energies indicates that silver mainly exists in the Ag^0 state on the as-milled C2BT powder surface.[35] SEM and EDX mapping of Ag for the C2BT-Ag powders are presented in Figure 5C and D, respectively. Although Ag particles could not be observed directly due to their extremely small sizes, their uniform distribution in C2BT powders is evident in EDX mapping. Accordingly, both XPS and EDX results confirm that metallic Ag nanoparticles were successfully deposited onto the C2BT powder surface.

UV-Vis absorption spectra of the C2BT powders are shown in Figure 6A. The vertical dash line defines the boundary between UV and visible light. There was few visible-light absorption at the wavelength range of 400-650 nm. On the contrast, there was a sharp increase in light absorption at the wavelength of <400 nm. Thus, the C2BT powders show a main absorption in the UV light range. Figure 6B shows the derived Tauc plot for the C2BT powders. The optical band gap (E_g) of the C2BT powders can be calculated by the Tauc equation[36]:

$$(ahv)^n = A\left(hv - E_g\right) \quad (1)$$

where a is the measured absorption coefficient, h is the Planck's constant, v is the frequency of light, and A is a proportional constant. n is 0.5 and 2 for indirect and direct band gap materials, respectively. E_g can be calculated from the tangent line in a plot of $(ahv)^n$ against photon energy. Based on fitting using Equation (1), E_g of the C2BT is estimated to be direct with a value of 3.2 eV. This value is very close to those reported values (~3.3 eV) for $Bi_4Ti_3O_{12}$, $BaBi_4Ti_4O_{15}$, and $BaTiO_3$. The similarity of the band gap in these materials is due to the common TiO_6 octahedra.[37]

The photocatalytic activity of the C2BT and C2BT-Ag powders was evaluated by RhB photodegradation under simulated solar light. Figure 6C shows the degradation profiles of these photocatalysts. After the C2BT powders were irradiated by UV-vis light for 4 hours, ~16% of RhB was degraded, which clearly confirms photocatalytic activity of C2BT powders. As demonstrated previously, the C2BT shows ferroelectric behaviour. As a result, the arisen internal electric field enables to separate photo-induced charge carriers effectively, and thus facilitates RhB photodegradation. When compared to pure C2BT powders, silver-modified C2BT powders had a much higher photocatalytic degradation rate. 50% of RhB was degraded under the same irradiation condition. The experimental data in Figure 6C were fitted into the pseudo-first-order kinetic model using Langmuir–Hinshelwood equation [Equation (2)]:

$$\ln C_0/C = kt \quad (2)$$

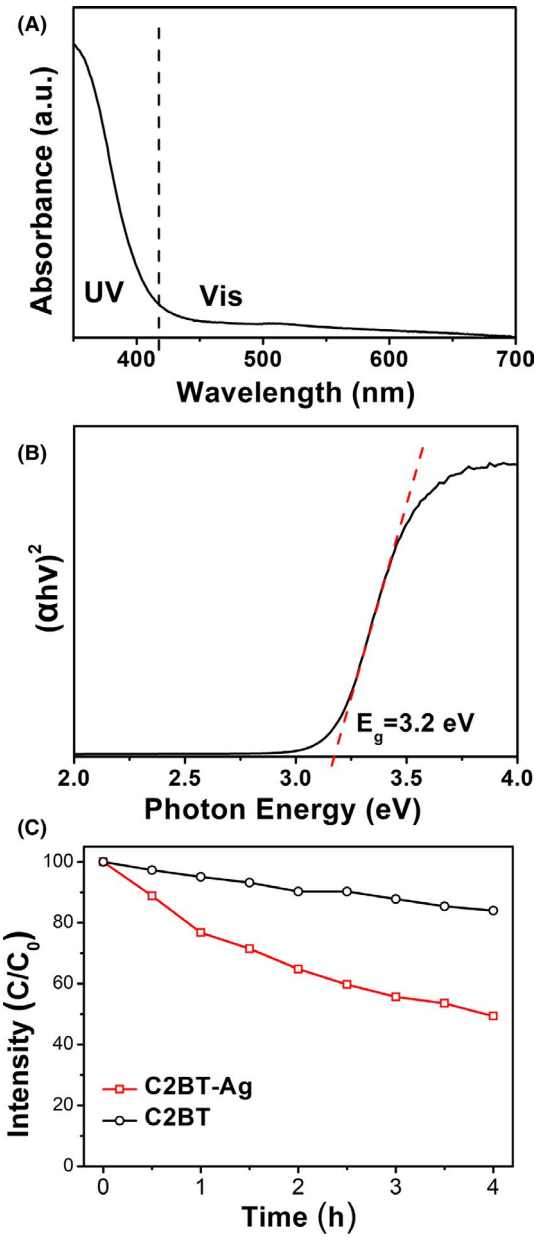

FIGURE 6 (A) UV-vis absorption spectrum of C2BT powders, where the dot line represents the boundary between UV and visible light; (B) The derived Tauc plot of C2BT, where the dot line traces the linear part; (C) Degradation profiles of RhB with C2BT and C2BT-Ag under solar simulator (100 mW/cm^2) [Color figure can be viewed at wileyonlinelibrary.com]

where C_0 and C are the initial concentration of RhB and the concentration at different irradiation time t, respectively, and k is the pseudo-first-order rate constant of photo degradation (min^{-1}).[38] The values of rate constant, which were determined from the slopes of the linear fits, are 0.0426 and 0.1724 min^{-1} for C2BT and C2BT-Ag photocatalysts, respectively. Thus, the rate constant of Ag-modified C2BT in RhB degradation is four times higher than that of pure C2BT. As a noble metal with excellent electronic conductivity, Ag can act as "electron traps" when deposited on the C2BT powder surface. This can enhance

the separation of photoexcited electrons and holes, and thus increase the photocatalytic activity of C2BT-Ag.[22,30,31]

4 | CONCLUSIONS

Aurivillius phase $Ca_2Bi_4Ti_5O_{18}$ (C2BT) powders with micrometer size were successfully prepared by the conventional solid-state reaction. To better understand photocatalytic activity, the crystal structure, dielectric, ferroelectric, and piezoelectric properties of C2BT were re-investigated. XRD indicated the material has polar orthorhombic structure with space group of *B2cb*. Although the onset of ferroelectric domain switching was not observed during *P-E* and *I-E* hysteresis loops measurement, frequency independent dielectric anomaly was detected at 774°C. After C2BT pellets were poled at 200°C, the d_{33} value of 0.7 ± 0.2 pC/N was obtained. Both frequency independent dielectric anomaly and detectable d_{33} value clearly indicated that C2BT is a ferroelectric with Curie point of 774°C. UV-vis spectrum showed that the C2BT powders had a UV light absorption and the derived Tauc plot suggested a direct band gap of 3.2 eV. Under simulated solar light irradiation for 4 hours, 16% of RhB solution was degraded with the presence of C2BT powders. When decorated with Ag nanoparticles on the surface of C2BT powders, 50% of RhB was degraded in the same condition. The rate constants of photo degradation were 0.0426 and 0.1724 min^{-1} for C2BT and C2BT-Ag photocatalysts, respectively. Above results demonstrate that C2BT exhibits photocatalytic activity due to its semiconducting and ferroelectric nature. The deposition of Ag nanoparticles on the C2BT powder surface significantly improved photocatalytic activity. To the best of our knowledge, we reported frequency independent dielectric anomaly, band gap value and photocatalytic properties of C2BT for the first time. This work shows great potential in developing novel photocatalysts with Aurivillius phase.

ACKNOWLEDGMENT

Dr Yaqiong Wang, Man Zhang, and Zimeng Hu would like to acknowledge the Chinese Scholarship Council for supporting this work.

ORCID

Yaqiong Wang https://orcid.org/0000-0002-0992-9479
Man Zhang https://orcid.org/0000-0002-1094-7279

REFERENCES

1. Suarez DY, Reaney IM, Lee WE. Relation between tolerance factor and Tc in Aurivillius compounds. J Mater Res. 2001;16(11):3139–49.
2. Zhou Z, Dong X, Yan H. Lanthanum distribution and dielectric properties of $Bi_{3-x}La_xTiNbO_9$ bismuth layer-structured ceramics. Scr Mater. 2006;55(9):791–4.
3. Yan H, Li CE, Zhou JG, Zhu WM. Structures and properties of bismuth layer-structured piezoelectric ceramics with high Tc. J Inorg Mater. 2000;15(2):209–20.
4. Park BH, Kang BS, Bu SD, Noh TW, Lee J, Jo W. Lanthanum-substituted bismuth titanate for use in non-volatile memories. Nature. 1999;401(6754):682–4.
5. Damjanovic D. Materials for high temperature piezoelectric transducers. Curr Opin Solid State Mater Sci. 1998;3(5):469–73.
6. Moure A. Review and perspectives of aurivillius structures as a lead-free piezoelectric system. App Sci. 2018;8(1):62.
7. Kikuchi T. Stability of layered bismuth compounds in relation to the structural mismatch. Mater Res Bull. 1979;14(2):1561–9.
8. Frit B, Mercurio JP. The crystal chemistry and dielectric properties of the Aurivillius family of complex bismuth oxides with perovskite-like layered structures. J Alloys Compd. 1992;188(1–2):27–35.
9. Aurivillius B, Fang PH. Ferroelectricity in the compound $Ba_2Bi_4Ti_5O_{18}$. Phys Rev. 1962;126(3):893–6.
10. Subbarao EC. A family of ferroelectric bismuth compounds. J Phys Chem Solids. 1962;23(6):665–76.
11. Fernandez JF, Caballero AC, Villegas M. Relaxor behavior of $Pb_xBi_4Ti_{3+x}O_{12+3x}$ (x= 2, 3) Aurivillius ceramics. Appl phys lett. 2002;81(25):4811–3.
12. Zhang S, Chen Y, Sun H, Pan X, Liu Z, Ming N. Epitaxial growth and dielectric properties of homologous $Sr_{m-3}Bi_4Ti_mO_{3m+3}$ (m=3, 4, 5, 6) thin films. Appl Phys Lett. 2001;81(26):5009–11.
13. Li X, Ju Z, Li F, Huang Y, Xie Y, Fu Z, et al. Visible light responsive $Bi_7Fe_3Ti_3O_{21}$ nanoshelf photocatalysts with ferroelectricity and ferromagnetism. J Mater Chem A. 2014;2(33):13366–72.
14. Ismunandar KT, Hoshikawa A, Zhou Q, Kennedy BJ, Kubota Y, Kato K. Structural studies of five layer Aurivillius oxides: A2Bi4Ti5O18 (A=Ca, Sr, Ba and Pb). J Solid State Chem. 2004;177(11):4188–96.
15. Moure C, Gil V, Tartaj J, Duran P. Crystalline structure, dielectric and piezoelectric properties of bismuth-layer $Ca_xBi_4Ti_{3+x}O_{12+3x}$ (x= 1, 2) compounds. J Eur Ceram Soc. 2005;25(12):2447–51.
16. Hou R, Chen X. Synthesis and dielectric properties of layer-structured compounds $A_{n-3}Bi_4Ti_nO_{3n+3}$ (A= Ba, Sr, Ca) with n> 4. J Mater Res. 2005;20(9):2354–9.
17. Xu Z, Chu R, Hao J, Zhang Y, Chen Q, Zhao L, et al. Study on high temperature performances for bismuth layer-structured $(Sr_{1-x}Ca_x)_2Bi_4Ti_5O_{18}$ ceramics. J Alloys Compd. 2009;487(1–2):585–90.
18. Sun S, Wang W, Xu H, Zhou L, Shang M, Zhang L. $Bi_5FeTi_3O_{15}$ hierarchical microflowers: hydrothermal synthesis, growth mechanism, and associated visible-light-driven photocatalysis. J Phys Chem C. 2008;112(46):17835–43.
19. Jang JS, Yoon SS, Borse PH, Lim KT, Hong TE, Jeong ED, et al. Synthesis and characterization of Aurivillius phase $Bi_5Ti_3FeO_{15}$ layered perovskite for visible light photocatalysis. J Ceram Soc Jpn. 2009;117(1371):1268–72.
20. Lin X, Lv P, Guan Q, Li H, Zhai H, Liu C. Bismuth titanate microspheres: directed synthesis and their visible light photocatalytic activity. Appl Surf Sci. 2012;258(18):7146–53.
21. Kim HG, Hwang DW, Lee JS. An undoped, single-phase oxide photocatalyst working under visible light. J Am Chem Soc. 2004;126(29):8912–3.

22. Cui Y, Briscoe J, Dunn S. Effect of ferroelectricity on solar-light-driven photocatalytic activity of $BaTiO_3$ influence on the carrier separation and stern layer formation. Chem Mater. 2013;25(21):4215–23.
23. Karthikeyan C, Arunachalam P, Ramachandran K, Al-Mayouf AM, Karuppuchamy S. Recent advances in semiconductor metal oxides with enhanced methods for solar photocatalytic applications. J Alloys Compd. 2020;828:154281.
24. Chen F, Huang H, Guo L, Zhang Y, Ma T. The role of polarization in photocatalysis. Angew Chem Intl Ed. 2019;58(30):10061–73.
25. Naresh G, Mandal TK. Excellent sun-light-driven photocatalytic activity by Aurivillius layered perovskites, $Bi_{5-x}La_xTi_3FeO_{15}$ (x= 1, 2). ACS Appl Mater Inter. 2014;6(23):21000–10.
26. Naresh G, Mandal TK. Efficient COD removal coinciding with dye decoloration by five-layer aurivillius perovskites under sunlight-irradiation. ACS Sustain Chem Eng. 2015;3(11):2900–8.
27. Jakob M, Levanon H, Kamat PV. Charge distribution between UV-irradiated TiO_2 and gold nanoparticles: determination of shift in the Fermi level. Nano Lett. 2003;3(3):353–8.
28. Gomes SC, Juárez R, Marino T, Molinari R, García H. Influence of excitation wavelength (UV or visible ligh on the photocatalytic activity of titania containing gold nanoparticles for the generation of hydrogen or oxygen from water. J Am Chem Soc. 2011;133(3):595–602.
29. Linic S, Christopher P, Ingram BD. Plasmonic-metal nanostructures for efficient conversion of solar to chemical energy. Nat Mater. 2011;10(12):911–21.
30. Qi W, Wang Y, Wu J, Hu Z, Jia C, Viola G, et al. Relaxor behaviour and photocatalytic properties of $BaBi_2Nb_2O_9$. J Am Ceram Soc. 2019;103(1):28–34.
31. Qi W, Wang Y, Wu J, Hu Z, Jia C, Zhang H. Relaxor ferroelectric and photocatalytic properties of $BaBi_4Ti_4O_{15}$. Adv Appl Ceram. 2019;118(7):418–24.
32. Xiong W, Porwal H, Luo H, Araullo-Peters V, Feng J, Titirici MM, et al. Photocatalytic activity of 2D nanosheets of ferroelectric Dion-Jacobson compounds. J Mater Chem. A. 2020;8(14):6564–8.
33. Chakrabarti A, Bera J. Effect of La-substitution on the structure and dielectric properties of $BaBi_4Ti_4O_{15}$ ceramics. J Alloys Compd. 2010;505(2):668–74.
34. Horiuchi S, Nagata H, Takenaka T. Piezoelectric properties of $Sr_2Bi_4Ti_5O_{18}$–$Ca_2Bi_4Ti_5O_{18}$ solid solution ceramics. Ferroelectrics. 2005;324(1):3–9.
35. Liu J, Sun Y, Li Z. Ag loaded flower-like $BaTiO_3$ nanotube arrays: fabrication and enhanced photocatalytic property. Cryst Eng Comm. 2012;14(4):1473–8.
36. Tauc J, Grigorovici R, Vancu A. Optical properties and electronic structure of amorphous germanium. Phys Status Solidi B. 1966;15(2):627–37.
37. Ehara S, Muramatsu K, Shimazu M, Tanaka J, Tsukioka M, Mori Y, et al. Dielectric properties of $Bi_4Ti_3O_{12}$ below the Curie temperature. Jpn J Appl Phys. 1981;20(5):877–81.
38. Kandi D, Martha S, Thirumurugan A, Parida KM. Modification of BiOI microplates with CdS QDs for enhancing stability, optical property, electronic behavior toward rhodamine B decolorization, and photocatalytic hydrogen evolution. J Phys Chem C. 2017;121(9):4834–49.

How to cite this article: Wang Y, Zhang M, Wu J, Hu Z, Zhang H, Yan H. Ferroelectric and photocatalytic properties of Aurivillius phase $Ca_2Bi_4Ti_5O_{18}$. *J Am Ceram Soc*. 2021;104:322–328. https://doi.org/10.1111/jace.17466